FIELD-ANALYSIS MODEL FOR PREDICTING DISPERSION PROPERTY OF COUPLED-CAVITY CIRCUITS

Fa Dai and Abbas S. Omar

Arbeitsbereich Hochfrequenztechnik
Technische Universität Hamburg-Harburg
D-2100 Hamburg 90, Germany

ABSTRACT

Based upon the generalized mode-analysis technique, a rigorous numerical model for simulating 'cold'-tests of millimeter wave coupled-cavity slow-wave circuits is developed. This model provides not only the dispersion property but also the 'cold' RF field distribution in the structure. The result is compared with that obtained by Curnow's equivalent circuit.

I. INTRODUCTION

An important characteristic in the design of slow-wave structures(SWS) for travelling-wave tubes(TWT's) is the dispersion property or k_0d-βd diagram. This diagram provides the necessary information about the phase and group velocities of different space harmonics and about the bandwidth of the SWS. Such characteristic is normally achieved from the 'cold'-test measurements, which are made on resonant sections of the structure with standard techniques such as perturbation method [1]. However, a series of 'cold'-test measurements has to be performed in order to investigate the effects of changes in structure dimensions on the tube performance, which is time-consuming and expensive. On the other hand, the cold tests and other simulatution models so far [2-6] cannot provide the information about the *RF* field distribution in the SWS, which is important for investigating the beam-wave interaction mechanism. Direct calculation of the *RF* field patterns is difficult because of the complexity of the shapes involved [2-4]. It is highly desirable to develop some analytic techniques to predict the properties of the SWS without repeating the expensive cold tests, but from economical numerical simulations. In this connection a field analysis model is developed, which is based on efficient mode expansions in each guide considered and matching them at the waveguide junctions in terms of generalized mode-matching technique [7-8]. The model can therefore provide not only the dispersion property of the SWS but also the information about the 'cold' *RF* field in the cavity. The result of this model for a typical structure is compared with that obtained by the equivalent circuit method. The good agreement is shown. The *RF* field patterns at abrupt junctions, being of the most difficulty of computations, are drawn. The convergence and consistence of the field patterns demonstrated the accuracy of the numerical solutions.

II. SCATTERING PARAMETERS OF PERIODIC UNIT

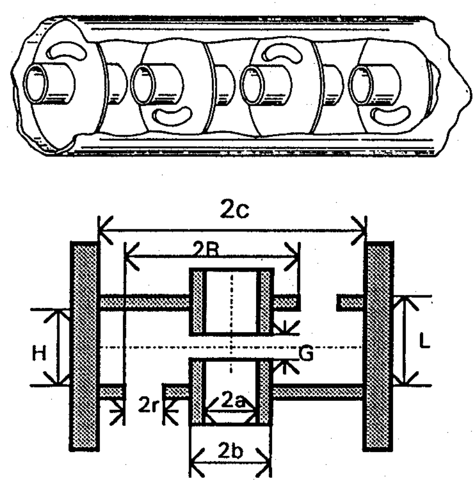

Fig.1 Sapce harmonic coupled-cavity slow-wave structure and its dimensions.

The coupled-cavity structure under consideration is shown schematically in Fig.1, which can be divided into several individual waveguides. The end view of the kidney-like coupling slot resembles a sector segment,

CH3277-1/93/0000-0901$01.00 © 1993 IEEE

which is thereby simplified to a sector waveguide. The angle of the sector is chosen to give the same area as the slot aperture, illustrated in Fig.2. Then, $\theta = \alpha + \frac{\pi r}{2R}$. The coupled-cavity thus consists of three types of individual cylindrical waveguides, i.e., circular-, coaxial-, and sector-waveguides, whose eigenmodes can be found out by solving Helmholtz equation combined with boundary conditions.

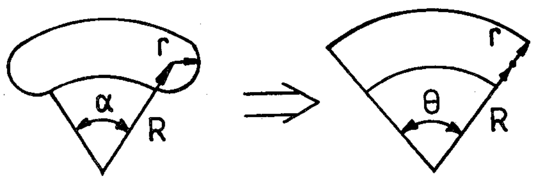

Fig.2 Coupling slot and sector waveguide.

The abrupt junctions in the coupled-cavity are normally concerned with two waveguides except for a kind of multiguide junctions between a circular waveguide and a coaxial waveguide with hollow inner conductor. The electromagnetic scattering problem at waveguide junctions can be solved by means of the generalized scattering matrix of the mode-matching technique [7-8]. Considering a typical multiguide junction, the so called k-furcated guide discontinuity, the transverse electric and magnetic fields can be expanded as the following matrix equations

$$\begin{cases} \vec{E}_t^{(i)} = [\mathbf{e}^{(i)}] \cdot \left([\lambda^{(i)}] \cdot [a^{(i)}] + [\lambda^{(i)}]^{-1} \cdot [b^{(i)}] \right), \\ \vec{H}_t^{(i)} = [\mathbf{h}^{(i)}] \cdot \left([\lambda^{(i)}] \cdot [a^{(i)}] - [\lambda^{(i)}]^{-1} \cdot [b^{(i)}] \right), \end{cases} \quad (1)$$

where the superscripts 'i' denote the ith guide, $i = I, 1, 2, \cdots, k$; $[a]$ and $[b]$ are column vectors with elements of complex amplitude a_m of the mth incident mode and b_m of the mth scattered mode, respectively; M means the number of expansion modes, $m = 1, 2, \cdots, M$; $[\lambda]$ is an $(M\text{x}M)$ diagonal matrix with elements $exp(-\gamma_m z)$, $\gamma_m = \alpha_m + \beta_m$ means propagation constant of the mth mode; $[\mathbf{e}]$, $[\mathbf{h}]$ are row eigenmode-vectors with elements $\vec{\mathbf{e}}_m, \vec{\mathbf{h}}_m$. Considering the continuity of transverse electric and magnetic fields on the junction plane z=0, we obtain a matrix representation of boundary conditions:

$$\begin{cases} [a^{(I)}] + [b^{(I)}] = [R]\left([b^{(II)}] + [a^{(II)}]\right) \\ [b^{(II)}] - [a^{(II)}] = [B]\left([a^{(I)}] - [b^{(I)}]\right). \end{cases} \quad (2)$$

where the detailed definitions of the matrices in (2) are given in [8]. Considering the multiguide junction as a generalized two-port discontinuity between guides 'I' and 'II' (= $1, 2, \cdots, k$,), the relations among the incident and scattered modes can be expressed by the scattering matrix representation as

$$\begin{aligned} \begin{bmatrix} b^{(I)} \\ b^{(II)} \end{bmatrix} &= \begin{bmatrix} S_{11} & S_{12} \\ S_{21} & S_{22} \end{bmatrix} \cdot \begin{bmatrix} a^{(I)} \\ a^{(II)} \end{bmatrix} \\ &= \begin{bmatrix} [\mathrm{I}]-[\mathrm{D}] & [\mathrm{D}][\mathrm{R}] \\ [\mathrm{B}][\mathrm{D}] & [\mathrm{I}]-[\mathrm{B}][S_{12}] \end{bmatrix} \cdot \begin{bmatrix} a^{(I)} \\ a^{(II)} \end{bmatrix} \end{aligned}, \quad (3)$$

where the matrix [D] is defined as $[D] = 2([\mathrm{I}] + [R][B])^{-1}$, an $(\mathrm{M}^{(I)} \times \mathrm{M}^{(I)})$ matrix. If the section 'II' contains only one waveguide, it is referred to as two-port discontinuity and the scattering matrix in (3) degenerates into the expression for two-port junction [7]. The combined S-matrix for cascaded discontinuities can be obtained by using equation (12) for a two-port junction in [7] and equation (18) for a multiguide junction in [8]. Thus the individual scattering matrices can be cascaded, one by one for each abrupt junction and waveguide line. Each step in the procedure can be examined by plotting the field-patterns and checking the boundary conditions required. It is also possible to give the detailed information about RF field at any position of the structure, provided the operation mode is known, which gains an advantage over other simulation models. For the multiguide junction related to a coaxial waveguide and two circular waveguides, the scattering parameters can be found out.

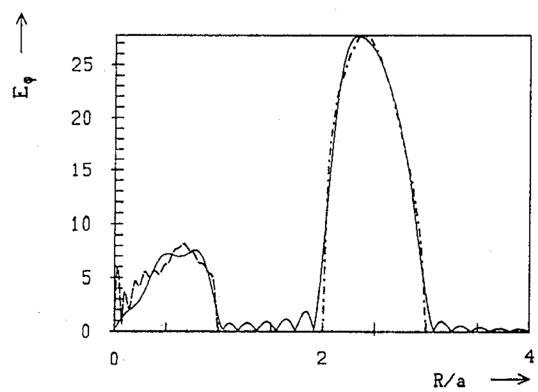

Fig.3 Transverse field component E_ϕ along r-axis at both sides of a circular-coaxial-circular junction, with TM_{21}/ESM/λ=5a incidence from '1'. CPU time 2.5 min with 40 modes used in each guide. '1': solid, a_1=4a, '2': dash dot, a_2=3a, b_2=2a, '3': dash a_3=a.

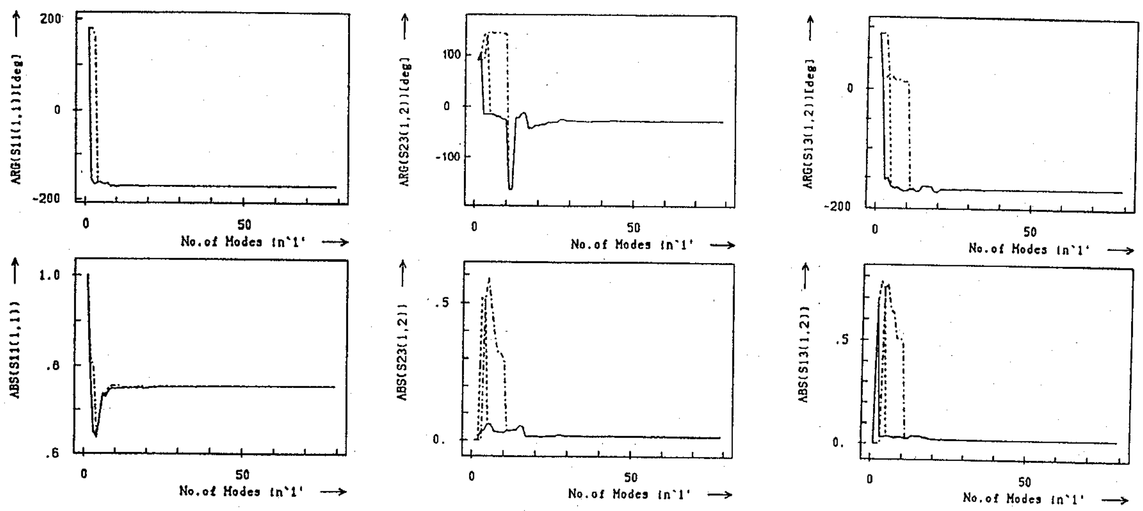

(a) Reflection Coefficient (b) Coupling Coefficient (c) Transmission Coefficient

Fig.4 Convergence of S-parameters versus the number of modes used in guide '1' for a circular-coaxial-circular junction, with TE_{11} incidence from '1'. Mode ratios used: $M^{(1)}:M^{(2)}:M^{(3)}$=1:1:1(solid), 1.5:1.2:1(dot), 4:3:1(dash dot). Guide dimensions: '1': $a_1=0.8\lambda$, '2': $a_2=0.6\lambda$, $b_2=0.4\lambda$, '3': $a_3=0.2\lambda$.

In order to check the accuracy of the boundary conditions required by the 3-guide junction, the transverse field component, taking E_ϕ as an example, are drawn in Fig.3, in which both the continuity and convergence of the field amplitudes are presented. Fig.4 gives the numerical results for reflection coefficient S_{11} in guide '1', transmission coefficient S_{13} from guide '1' to guide '3', and coupling coefficient S_{23} between guide '2' and guide '3' computed with different mode ratios. It shows a good convergence for all the three mode ratios, as 20 or more eigenmodes are used in guide '1'.

By cascading all the individual S-matrices in a periodic unit, in which eight abrupt junctions and eleven individual waveguides are involved, the overall S-matrix $S^{(u)}$ can be obtained. Thus the incident and scattered modes of nth and $(n+1)$th terminal planes of the periodc structure are related by

$$\begin{bmatrix} b_n \\ b_{n+1} \end{bmatrix} = \begin{bmatrix} S_{11}^{(u)} & S_{12}^{(u)} \\ S_{21}^{(u)} & S_{22}^{(u)} \end{bmatrix} \cdot \begin{bmatrix} a_n \\ a_{n+1} \end{bmatrix}. \tag{4}$$

III. DISPERSION EQUATION

Applying the Floquet's theorem to the periodic SWS, the incident and scattered waves at the nth and $(n+1)$th terminal planes can also be related by

$$\begin{bmatrix} b_n \\ b_{n+1} \end{bmatrix} = \begin{bmatrix} [0] & e^{\gamma d}[I] \\ e^{-\gamma d}[I] & [0] \end{bmatrix} \begin{bmatrix} a_n \\ a_{n+1} \end{bmatrix}, \tag{5}$$

where [I] is the unity matrix and d is the length of a periodic unit. Combining the matrix equations (4) and (5), one gets a matrix eigenvalue equation for the propagation constant γ:

$$\left(\begin{bmatrix} S_{11}^u & S_{12}^u \\ S_{21}^u & S_{22}^u \end{bmatrix} - \begin{bmatrix} [0] & e^{\gamma d}[I] \\ e^{-\gamma d}[I] & [0] \end{bmatrix} \right) \begin{bmatrix} a_n \\ a_{n+1} \end{bmatrix} = 0 \tag{6}$$

A nontrivial solution exists only if the determinant vanishes:

$$\begin{vmatrix} [S_{11}^u] & [S_{12}^u] - e^{\gamma d}[I] \\ [S_{21}^u] - e^{-\gamma d}[I] & [S_{22}^u] \end{vmatrix} = 0 \,. \tag{7}$$

The eigenvalue problem involved in the dispersion equation (6) or (7), which contains only the operation frequency and structure dimensions as variables, can be solved by using some standard routines from the programm libraries such as the *NAG library*. The basic dispersion property of the SWS can thus be plotted by running the frequency as a variable. In order to compare the results obtained by field analysis with that from equivalent circuit method, Curnow's lumped element equivalent circuit for coupled-cavity circuit [2] is employed. The circuit parameters have been related to the structure dimenstions by means of Carter's empirical formulations except to corrections for equation (2) in [4]. The coupling factor *k*, defined as the fraction of the circulating current of the cavity intercepted by a slot, should be that $k=\frac{\alpha}{2\pi}+\frac{r}{4R}$, where α is the slot sector angle illustrated in Fig.2. For a typical structure, Fig.6 shows the numerical results of k_0L-βL diagramm obtained by the field analysis (solid line) and the equivalent circuit (dashed line). The results obtained by both methods agree well with each other. For field-analysis model, the whole procedure to calculate one frequency can be carried out on a ***Convex*** computer within 10min of CPU time for 60 eigenmode used in each guide.Another important parameter for TWT simulations is the ***coupling impedance***, which represents the interaction intensity between the *RF* circuit field and the electron stream. According to the field expansion discussed above, the coupling impedance may be expressed as

$$\mathcal{K}_c=\frac{1}{2\beta^2}\sum_{n=1}^{\mathcal{M}}\left|\left(a_{ne}+b_{ne}\right)\frac{e_{zn}}{\sqrt{P_{ne}}}\right|^2 , \qquad (8)$$

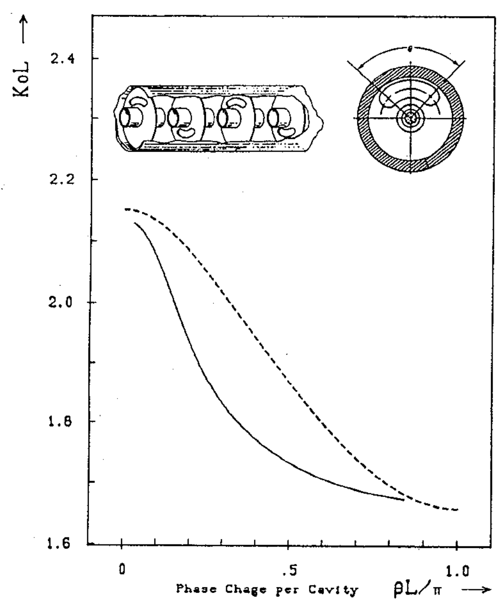

Fig.5 Dispersion property of a coupled-cavity cavity slow-wave structure obtained by field-analysis with 60 modes used in each waveguide (solid line) and equivalent circuit method (dashed line). Structure dimensions: *a*=2.55mm, *b*=3.2mm, *c*=7.63mm, *r*=1.4mm, θ=2.27, *R*=5.8mm, *G*=2.84mm, *H*=6.44mm, *L*=8.84mm.

where a_{ne} and b_{ne} are the expansion coefficients for forward and backward TM waves, P_{ne} is the normalized coefficient of the *n*th mode. Therefore, the coupling impedance at any position of a coupled-cavity SWS can be evaluated by the field analysis model.

IV. CONCLUSIONS

Based on the generalized mode-matching technique, a field analysis model for simulating 'cold'-test measurements of millimeter wave coupled-cavity *RF* circuits has been developed, which provides not only the dispersion and impedance properties of the periodic slow-wave structure but also the information about the 'cold' *RF* field in the cavity. The emphasis of the current work has been on efficiently simulating the frequency-phase characteristics, although a broader range of applications is envisioned. The results for a typical structure agreed with those obtained by the equivalent circuit method. With appropriate modifications, the model can be used effectively as design means for coupled-cavity TWT's.

V. REFERENCES

[1] D. J. Connolly, "Determination of the interaction impedance of coupled cavity slow wave structures," *IEEE Trans. Electron Devices,* vol. ED-23, pp. 491-493, May 1976.

[2] H.J. Curnow, "A general equivalent circuit for coupled-cavity slow-wave structures," *IEEE Trans. Microwave Theory Tech.,* vol. MTT-13, pp. 671-676, Sept. 1965.

[3] R.G. Carter, "Representation of coupled-cavity slow-wave structures by equivalent circuits," *IEE Proc.*, vol. 130, pt.I., no. 2, pp. 67-72, Apr. 1983.

[4] R.G Carter and S. Liu, "Method for calculating the properties of coupled-cavity slow-wave structures from their dimensions," *IEE Proc.*, vol. 133, pt.H., no.5, pp. 330-334, Okt. 1986.

[5] A.T. Drobot et al., "Numerical simulation of high power microwave sources," *IEEE Trans. Nucl. Sci.*, vol. NS-32, no.5, pp.2733-2737, Oct. 1988.

[6] P. Prince et al., "A numerical method for predicting brillouin plots of coupled-cavity circuits," *IEDM Tech, Dig. (San Francisco, USA.),* pp.676-679, Dec. 1984.

[7] A.S. Omar and K.F. Schuenemann, "Transmission matrix representation of finline discontinuities," *IEEE Trans. Microwave Theory Tech.*, vol. MTT-33, pp. 765-770, Sept. 1985.

[8] F. Dai, "Scattering and transmission matrix representations of multiguide junctions," *IEEE Trans. Microwave Theory Tech.,* vol. MTT-40, pp. 1538-1544, July. 1992.